Experimental investigation on the evaporation of a wet porous layer inside a vertical channel with resolution of the heat equation by inverse method

Amine Terzi, Walid Foudhil, Souad Harmand, Sadok Ben Jabrallah

Energy Conversion and Management 126 (2016) 158–167

Experimental investigation on the evaporation of a wet porous layer inside a vertical channel with resolution of the heat equation by inverse method

A. Terzi [a,b,*], W. Foudhil [a], S. Harmand [c], S. Ben Jabrallah [a,b]

[a] Laboratoire d'Energétique et des Transferts Thermique et Massique, Faculté des Sciences de Tunis, Campus Universitaire, 1060 Tunis, Université El Manar, Tunisia
[b] Faculté des Sciences de Bizerte, 7021 Bizerte, Université de Carthage, Tunisia
[c] Université de Lille Nord de France, F-59000 Lille UVHC/TEMPO, F-59313 Valenciennes Cedex, France

Keywords:
Evaporation
Porous layer
Inverse method
Heat and mass transfer

A b s t r a c t

In this paper, we realize an Experimental study of the evaporation of a wet porous layer inside a vertical channel. To develop this study, an experimental dispositive was realised. We measure the temperature along the plate and the evaporated flow rate using the test bed. From these measurements we note that the profiles of the temperature are divided into two areas: the heating and the evaporation zone. We also note that the use of the porous layer is more efficient for high heating flux and low liquid inlet flow. In addition, we studied different dimensionless numbers by solving the energy equation by inverse method. We note that the latent Nusselt number is more important than the sensible Nusselt Number, which proves that the flow dissipated by evaporation is greater than the one used by the film to increase its temperature.

1. Introduction

The phenomena of heat and mass transfer during the flow of a liquid film on a heated wall has a considerable interest in the engineering field, which was translated into many applications, such as the refrigeration [1], air conditioning [2], photovoltaic [3], energy-saving [4] and the cooling of electronic components. In order to understand the heat and mass transfer, different geometries were studied. Firstly, the flow of a liquid was examined on a horizontal flat plate [5]. We cite Siow et al. [6], who studied the evaporation of a laminar model within a horizontal channel. Yuan et al. [7] conducted a study on the coupled heat and mass transfer from a thin film of water subjected to a flow of moist air.

Thereafter, several studies addressed the case of a vertical plate in order to improve the flow of the liquid. Ben Jabrallah et al. [8] studied the coupled heat and mass transfer in a rectangular cavity that acts as a distillation cell. Cherif et al. [9] realised an experimental study on the natural and forced convection evaporation of a thin liquid film that flows on the inner faces of the plates of a vertical channel. Fahem et al. [10] conducted a numerical analysis on the heat and mass transfer within a distillation cell. Debbissi et al. [11] studied the evaporation of water by free and mixed convection into humid air and superheated steam. Min and Tang [12] conducted a theoretical study to analyze the characteristics of transient evaporation of a water film attached to an adiabatic solid wall.

Later on, other researchers have studied evaporation on an inclined plane [14–16,13], which affects gravitational forces and decreases the rate of fluid flow. We cite Zeghmati and Daguenet [17] who realised a study of transient laminar free convection over an inclined wet flat plate. Agunaoun and Daif [18] studied the evaporation of a thin film of water flowing on an inclined plate surface at a constant temperature that is higher than the air temperature.

From what was stated above, it is clear that researchers have studied different geometries and conducted parametric studies at almost all input parameters that may influence the heat and mass transfers.

On the other hand, alternative solutions, such as the use of binary fluids, have also been proposed to improve transfer. Cherif and Daif [19] conducted a numerical study on the heat and mass transfer between two vertical flat plates in the presence of a binary liquid film that flows on one heated plate. Debbissi et al. [20] studied the evaporation of a binary liquid film in a vertical channel.

However, obtaining a homogenous liquid film over the entire plate constitutes a major discrepancy between the theoretical and experimental studies. Despite efforts made in the field of modeling and numerical simulation, we still see a difference between calcu-

* Corresponding author at: Laboratoire d'Energétique et des Transferts Thermique et Massique, Faculté des Sciences de Tunis, Campus Universitaire, 1060 Tunis, Université El Manar, Tunisia.
E-mail address: terziamine@hotmail.fr (A. Terzi).

DOI : 10.1016/j.enconman.2016.07.085

Nomenclature

C_p	heat capacity at constant pressure [J kg^{-1} K^{-1}]
e	thickness of porous layer [m]
g	gravity acceleration [m s^{-2}]
h	heat transfer coefficient [W m^{-2} K^{-1}]
K	permeability [m^2]
L	length of the plate [m]
L_v	latent heat of water [J kg^{-1}]
m_{eV}	evaporating mass flow [kg s^{-1} m^{-2}]
Nu_L	latent Nusselt number [–]
Nu_s	sensible Nusselt number [–]
p	interne production [W m^{-3}]
q	heat flow [W m^{-2}]
T	temperature [K]
(x, y)	Cartesian coordinates [m]

Greek symbols

ρ	density [kg m^{-3}]
λ	thermal conductivity [W m^{-1} K^{-1}]
φ	heat flux density [W m^{-2}]

Subscripts

av	front
ar	back
eV	evaporated
in	entrance
T	total
L	latent
s	sensible
cd	conduction
p	plate
mes	measured
cal	calculated

lations and experiments. In a previous work, Cherif et al. [21], have studied the two aspects of the evaporation of a liquid film: experimental and numerical. A difference was reported. They believe that this difference is caused by the difficulty of making a falling film on a vertical plate. In fact, the film could not be controlled if it was directly adhered to the plate. To analyze the effect of dry zones on the plate, Debbissi et al. [22] realised a numerical study of the evaporation along an inclined plate. This plate is composed of two wet zones separated by a dry zone. The results of this study showed that the length of the dry zone plays an important role.

More recent studies have explored various techniques to solve this problem. For example, several researchers used rough surfaces, or interposed obstacles [23]. For example, Zheng and Worek [24] realised numerical and experimental studies on the evaporation of a liquid film inside an inclined channel. They fixed glass rods on the plate to disrupt the flow of liquid, thus improving the heat and mass transfer.

We believe that the best way to achieve a falling film on a flat plate and control its characteristics is the application of a porous layer that plays the role of a support for the liquid film. Few studies have theoretically examined the effect of the presence of a porous medium during evaporation [25,26] and as far as we now here is not an experimental study that have examined the case of a liquid film evaporation along a vertical plate that is covered with a porous layer. As a result, this work focuses on the study of the evaporation of a wet porous layer inside a vertical channel. The main objective of this study is to evaluate the variation of the temperature and the evaporated flow rate as well as to determine the best operating conditions for a better performance of the system. We have also solved the heat equation by inverse method to determine the local variation of the evaporated flow rate and thereafter the local variation of the latent and sensible Nusselt numbers.

2. Experimental facility

2.1. Setup

To conduct the study we realised an experimental setup which we represent in Figs. 1 and 2. It is composed of:

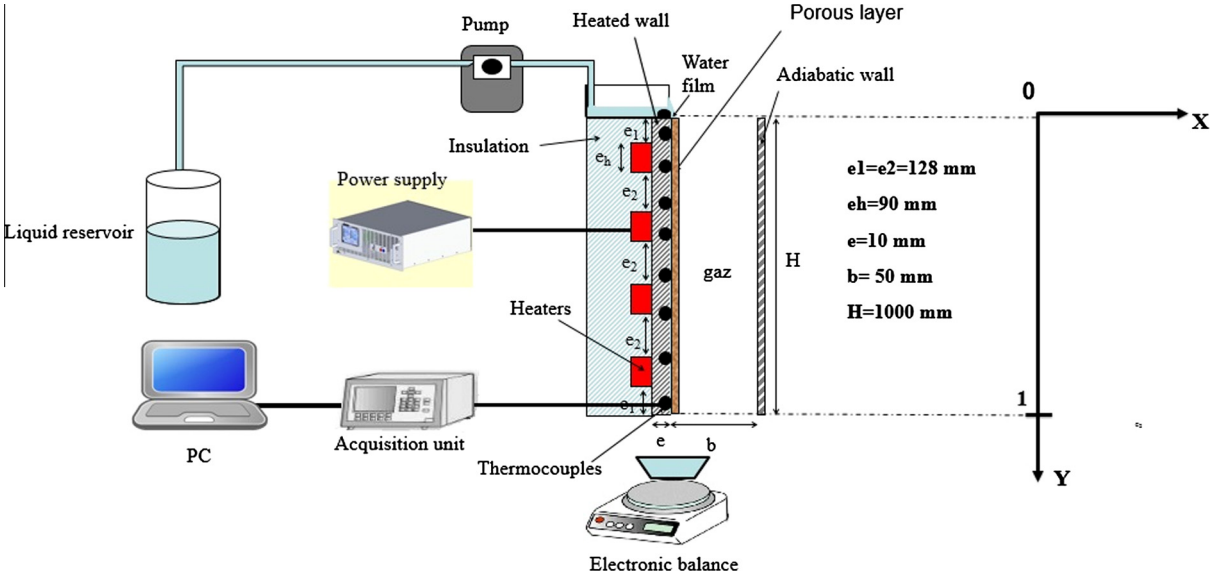

Fig. 1. Schematic presentation of the physical domain.

DOI : 10.1016/j.enconman.2016.07.085

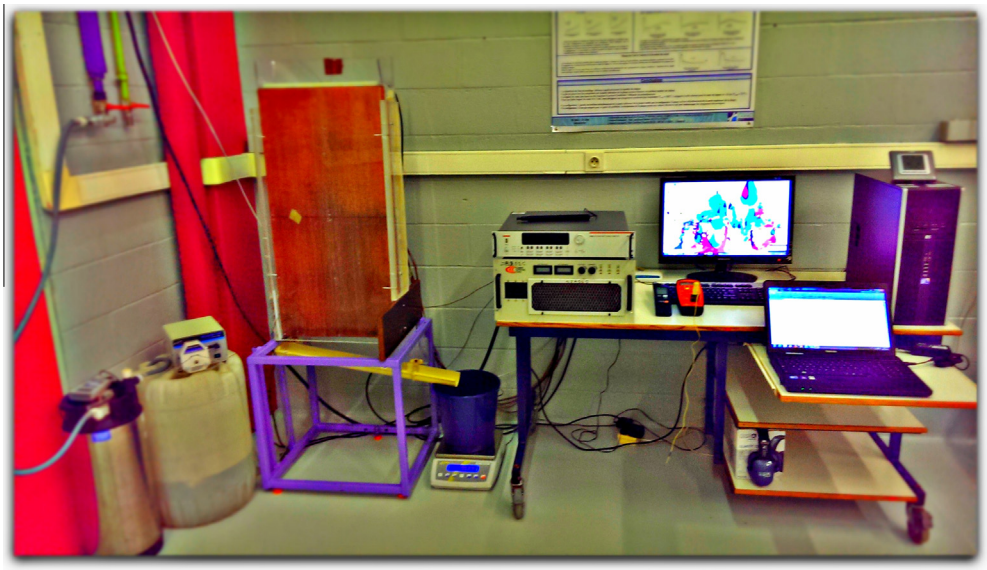

Fig. 2. The experimental device in real site.

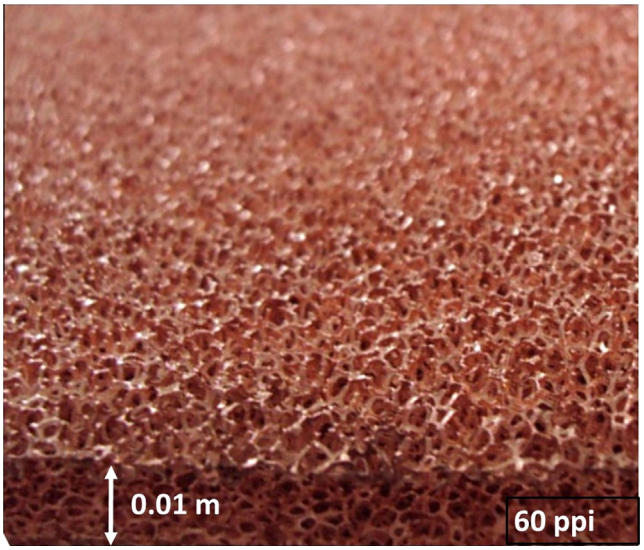

Fig. 3. The porous layer.

An aluminium plate which the dimensions are $1 \times 0.5 \times 0.012$ m. the front face of the plate was covered by a porous layer which is a copper metal foam represented in Fig. 3. Its caracteristiques are summarized in Table 1.

A heating system composed of 12 electrical resistors distributed homogeneously over the entire rear face of the plate and connected to a generator.

An isolation system composed of a glass wool layer and a plexiglas placed around the resistors to avoid the losses of energy.

A measurement system that allow the automatic acquisition of the temperature measured by differents thermocouples. In fact, for measuring the temperature 40 K-thermocouples with accuracy equal to $\Delta T = 0.05$ °C have been embedded along the aluminium plate. We represent in Figs. 4 and 5 a schematic laying of the thermocouples and their positions on real site successively.

A water supply system consisted of two water reservoir, a distiller, an electronic balance and a pump drive. Indeed, the distiller is used to minimize the limescale and impurities from the water. It provides continuous feed water to the first reservoir. The second reservoir is set above the plate, which once full, is drained by overflow, thus creating water film flowing homogeneously on the exchange surface. To have a fixed and stable mass flow rate, water circulates between the two reservoirs through a pump. The water flow at the outlet is measured using an electronic balance connected to a computer with accuracy equal to $\Delta m = 10^{-5}$ kg.

Table 1
Properties of the porous layer.

Properties	Values
Thickness	0.01 m
Thermal conductivity	390 W m^{-1} K^{-1}
Porosity	0.8
Permeability	$8.5 \cdot 10^{-8}$ m^{-2}

2.2. Error analysis

We have used the approach described by Barford [27], to estimate the uncertainties in the experimental results of this study. The overall uncertainty assigned to a given measurement is defined as the RSS (root-sum-square) combination of the fixed error. These errors are caused by the instrumentation in addition to the biased measurements. The measured experimental errors are ±2.5 °C for temperatures, ±0.46 g m^2 s^{-1} for water outlet and inlet flow, ±0.1 m s^{-1} for the velocity and ±12 W m^{-2} for the density heat flux. Table 2 summarize all the measurement uncertainties of the experimental results.

2.3. Measurements

Before beginning measurements, preliminary tests were performed to test the correct functioning of the device. First, the thermocouples were tested at ambient temperature, then under heating flows. We represent in Fig. 6 the variation of the local temperature along the vertical plate in natural convection without phase change (without liquid). For safety reasons and compliance with operating limits of heated components, we have chosen to study the case of natural convection only for a density heat flux equal to 800 W m^{-2}. Observing the figure, we note that the temperature increases from the bottom to the top of the plate. The area

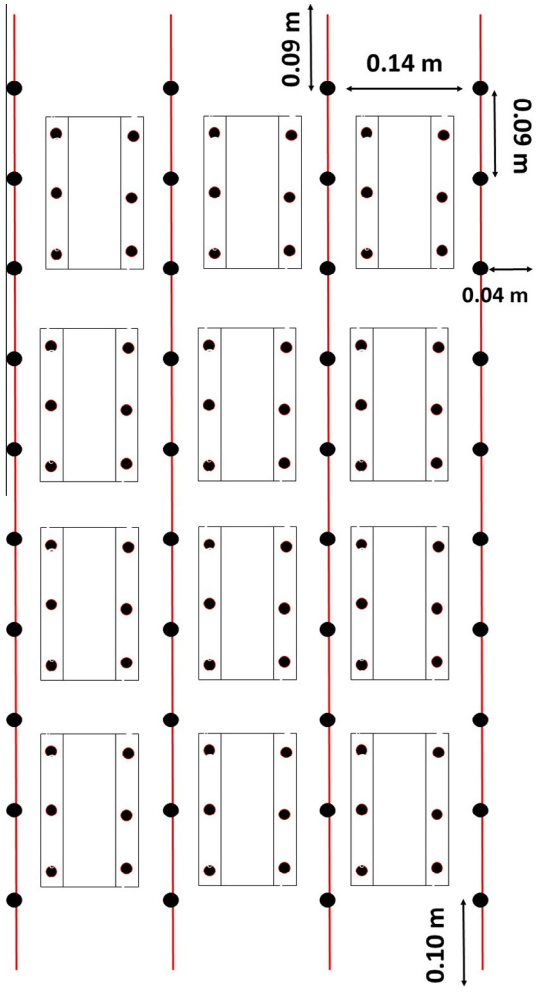

Fig. 4. The schematic laying thermocouple on the aluminium plate.

Table 2
Measurement uncertainties.

Variables	Uncertainty
Temperature	2.5 °C
Water outlet flow	0.46 g m^2 s^{-1}
Water inlet flow	0.46 g m^2 s^{-1}
Velocity	0.1 m s^{-1}
Density heat flux	12 W m^{-2}

near the plate is hotter, the density decreases and therefore creating an air flow near the plate. Fresh air is sucked towards the plate which explains this temperature difference between the upper area and the lower area of the plate.

After checking the correct functioning of the thermocouples and the heating system, we have verified the conservation of the water inlet flow in the outlet of the channel to ensure that there is no loss of water.

The density heat flux and the water inlet flow are important operating parameters. In fact, it is worthy to study their effects in the heat and mass transfer. Therefore, tests are realised with variant heating power from 400 W to 1400 W and using two water inlet flows ($m_{in} = 2.77$ g m^{-2} s^{-1} and $m_{in} = 4.44$ g m^{-2} s^{-1}). Table 3 contain the variation ranges of the experimental conditions.

3. Resolution of the heat equation by the inverse method

Certainly, knowing the temperature at any point of the wet wall requires special interest in understanding the phenomena of evaporation. But the knowledge of the local variation of the evaporated flow is essential. For that reason, and from the values of the measured temperatures, we must solve the heat equation on the plate. This resolution allows us to determine the values of the exchange coefficient at the wet wall and determine subsequently the variation of evaporated flow.

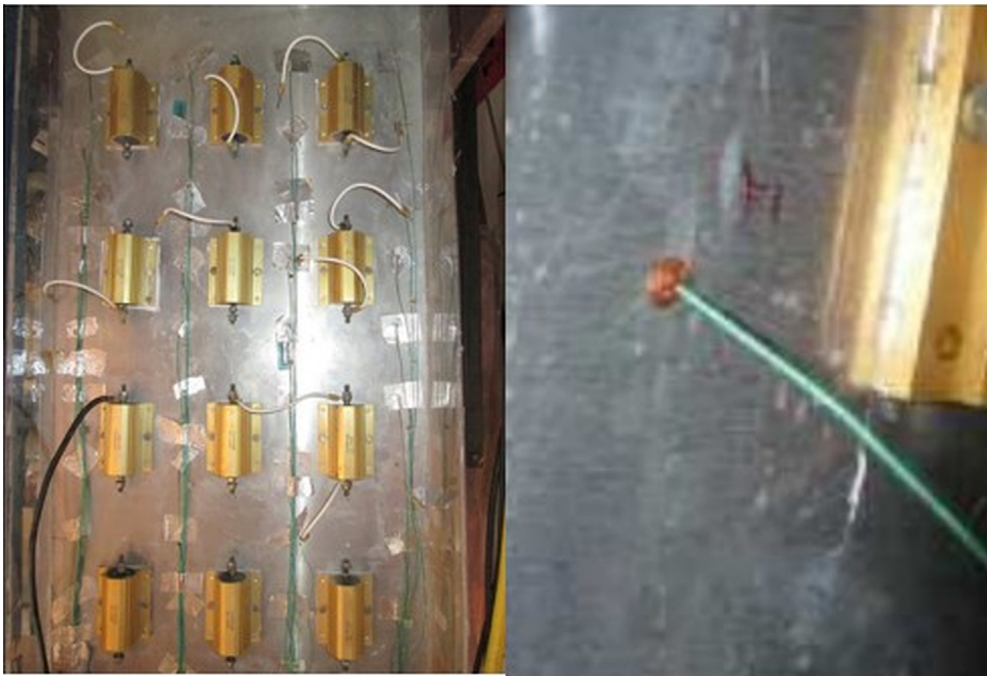

Fig. 5. The thermocouples in real site.

DOI : 10.1016/j.enconman.2016.07.085

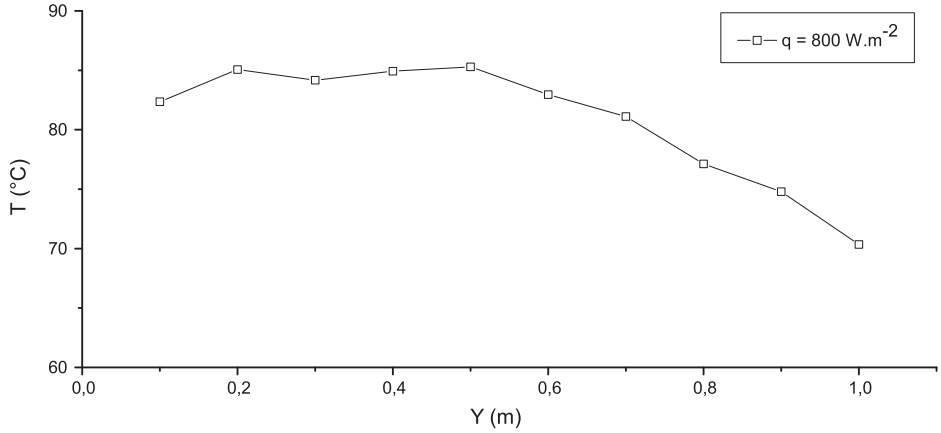

Fig. 6. Local variation of the temperature without liquid film.

Table 3
Variation range of the experimental conditions.

Variables	Minimum	Maximum
Ambient temperature (°C)	15	25
Inlet water temperature (°C)	15	22
Water inlet flow (g s^{-1} m^{-2})	2.77	4.44
Density heat flux (W m^{-2})	800	2800
Humidity (%)	40	65

3.1. Heat equation

The heat equation can be expressed by:

$$p(x,y) + \lambda \left(\frac{\partial^2 T}{\partial x^2} + \frac{\partial^2 T}{\partial y^2}\right) = \frac{1}{e}(\varphi_{ar} + \varphi_{av}) + \alpha\rho C_p \frac{\partial T}{\partial t} \quad (1)$$

where p is the intern production (W m^{-3}), assumed to be homogeneous throughout the electrical resistance. φ_{av} is the desired flux density corresponding to convection and radiations on the upper side of the resistor. First of all, we note that the back of the electrical resistance is isolated, which means that the flux density dissipated by the back is $\varphi_{ar} = 0$. Secondly, we will assume that the problem is stationary, so $\frac{\partial T}{\partial t} = 0$.

The equation takes the following form:

$$p(x,y) + \lambda \left(\frac{\partial^2 T}{\partial x^2} + \frac{\partial^2 T}{\partial y^2}\right) = \frac{1}{e}\varphi_{av} \quad (2)$$

The problem is a priory well-posed, since it has only a single unknown, which is the conductive flux, and could therefore be the subject of a direct resolution. But the problem is determining with accuracy the conductive flow in the resistance from the temperatures experimentally measured, which are noisy. The right way is to implement an inverse resolution for this problem. More precisely the flow is determined by solving an inverse conduction problem, coupled with the direct thermal modeling of the general equation shown above, by finite differences.

3.2. Inverse method

3.2.1. Principle of the method

A direct problem consists in the determination of the effects from the knowledge of causes. An inverse problem is the determination of the causes that led to those known effects. These methods are used in thermal studies to determine unknown physical properties such as conductivity or the boundary conditions for example the conductive flux [28–30]. For our problem, the flux is determined by solving an inverse conduction problem, coupled with the direct thermal modeling of the general equation shown above, by finite differences. The principle of the inverse method consists in the correction of the flux imposed from the comparison between temperatures measured by thermocouples and the numerically calculated temperatures. Therefore, the research process of the conductive flux is iterative. However, the solution is very sensitive to changes, even small ones, in the input data (geometry, material properties, the boundary conditions, ...). These uncertainties are inevitable given the uncertainties that

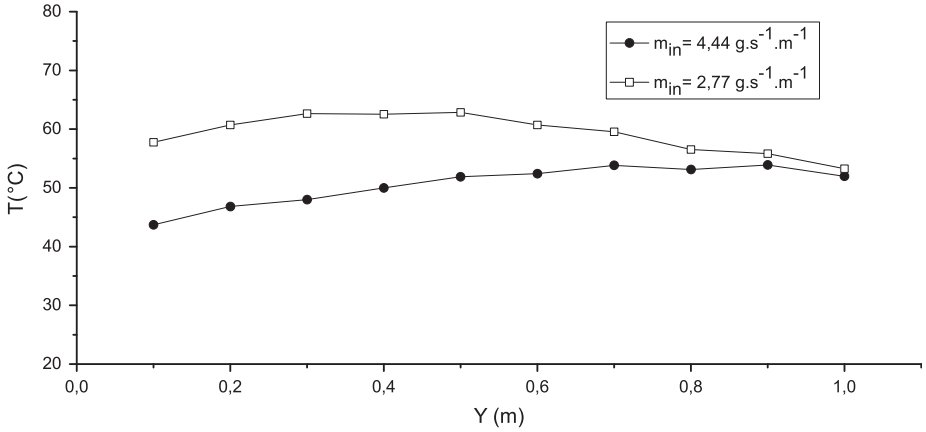

Fig. 7. Local variation of the temperature throughout the plate for different liquid inlet flow ($q = 800$ W m^{-2}).

may exist in the measures. The successive iterative search process can amplify uncertainties in the input data, therefore it increases the error in the result. In this case, the problem is ill-posed [31]. To make the search process more stable, we usually use a regularization method [32] which limits the effect of these uncertainties on the result [33].

3.2.2. Method of regularization

In order to correctly determine the flow corresponding to the temperatures measured experimentally, as mentioned above, we must narrow the difference between the temperatures calculated by direct method and measured temperatures to reach 0. Thus we aim to minimize the following criterion:

$$F = \sum_x \sum_y (T_{cal}(x,y) - T_{mes}(x,y))^2 \quad (3)$$

The minimization of this criterion alone does not regulate research and allows the amplification of errors in input data. Thus, we follow the method described by Beck [34]. It consists in adding the regularization terms to the previous criterion, and therefore we get:

$$F = \sum_x \sum_y (T_{cal}(x,y) - T_{mes}(x,y))^2 + \alpha \sum_x \sum_y (grad(\varphi_{av}(x,y)))^2 \quad (4)$$

4. Results and discussions

During the tests, the effect of water inlet flow rate was examined. To analyze its influence, we present in Fig. 7 the local variation of temperature for two water inlet flows $m_{in} = 2.77$ g m^{-2} s^{-1} and $m_{in} = 4.44$ g m^{-2} s^{-1}.

First of all, we note that the temperature profiles are divided into two areas. The first area starts at the top of the plate ($Y = 0$) to the point where the temperature reaches its maximum. In this part of the plate, the water film receives a sensible heat flux which increases the liquid temperature linearly: It is the heating zone. From the point where the temperature reaches its maximum to the bottom of the plate, we note that the temperature of the plate becomes almost constant and even decreasing. Indeed, in this second zone, the heat flow received by the liquid is fully used in the evaporation process as a latent heat: It is the evaporation zone. This result is proved in the work of Ben Jabrallah et al. [8] who has demonstrated the existence of these two zones in the case of the evaporation of a liquid film flowing on the wall of a vertical cavity. Secondly, for low inlet water flow, the measured temperatures are higher. Indeed, increasing the water inlet flow rate causes an increase in the film thickness and therefore its thermal resistance. Thus, the flow evacuated by the plate towards the liquid film is more important for a low flow rate. In the other hand, we note that the temperature differences for both inlet water flow are important in the entrance of the channel. These differences decrease in the output. As mentioned above, this second zone is characterized by a latent energy transfer. The entire heat flux transferred from the plate to the film is consumed by the process of evaporation, which explains the narrowing gaps in this area.

The density heat flux is an important parameter that is worth investigating. We represent in Fig. 8, the evolution of the temperature along the plate for different density heat flux. Firstly, it is

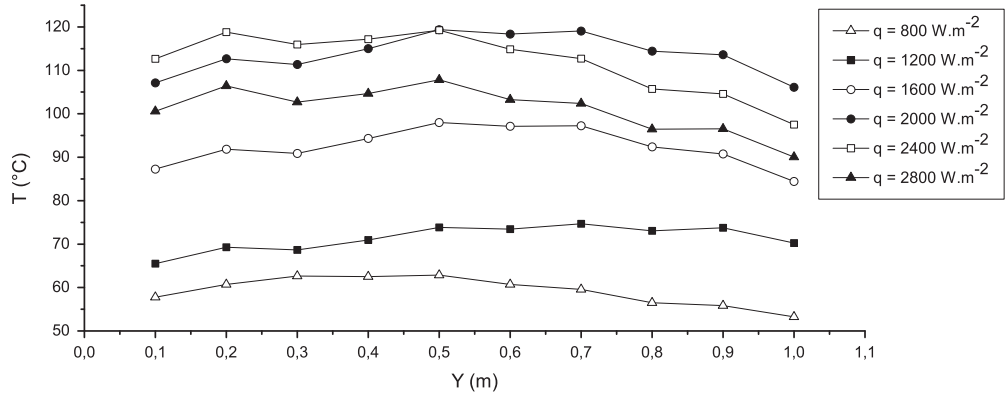

Fig. 8. Local variation of the temperature throughout the plate for different density heat flux ($m_{in} = 2.77$ g m^{-2} s^{-1}).

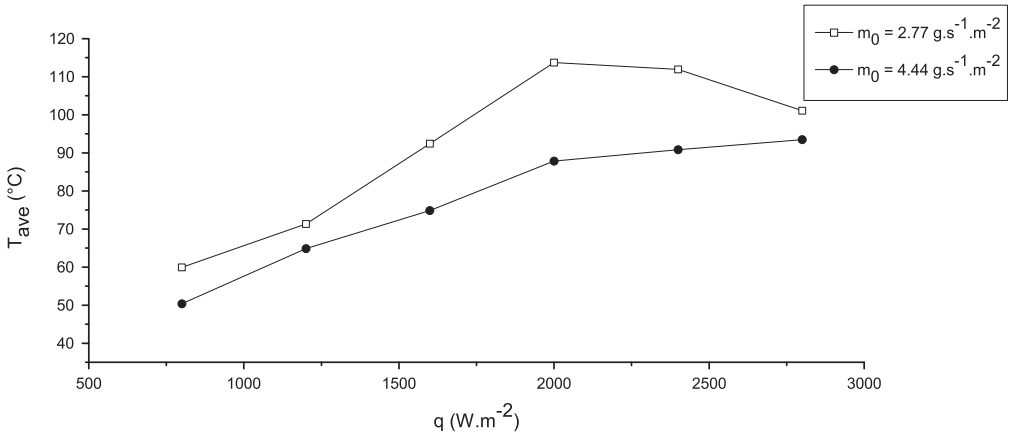

Fig. 9. Variation of the average temperature.

DOI : 10.1016/j.enconman.2016.07.085

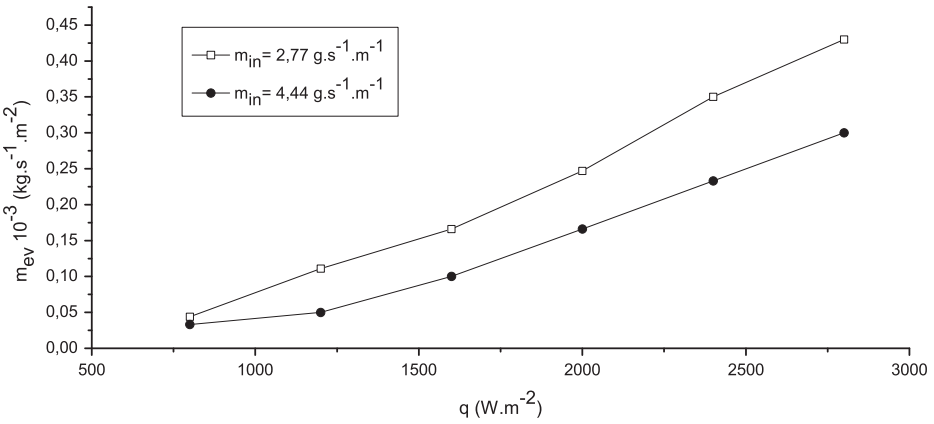

Fig. 10. Variation of the average evaporated flow rate.

noted that the temperature increases along with the heat flows, which is in agreement with most previous works [8–10,25,26], but, Beyond 2000 W m^{-2} the phenomenon is reversed and the temperature decreases with increasing the heat flux. To better visualize this phenomenon, we have presented in Fig. 9 the variation of the average temperature for different heat flux density. We see that the maximum of the temperature is obtained for a heat flux that is equal to 2000 W m^{-2}. Beyond this value, the temperature decrease. To understand this phenomenon and find an explanation for this temperature decrease, we present in Fig. 10 the variation of the global evaporated flow rate for different heat flux density. We note that the evaporated rates become important for a high heat flux. The phase change consumes a large quantity of energy, which explains the decrease in temperature. So we can conclude that the use of the porous layer is more efficient for high heat flow.

Fig. 11 shows the local variation of the evaporated flow along the plate for different heat flows and different liquid inlet flows. The heat flow is the essential source of energy needed to the liquid-gas change phase. By observing the variation of the evaporated flow, we find that an increase in the heat flow leads to an improved evaporated flow. Indeed, an increase in the heating density generate an energy addition which results in thermal and mass gradients increases. On the other hand, we see that increasing the

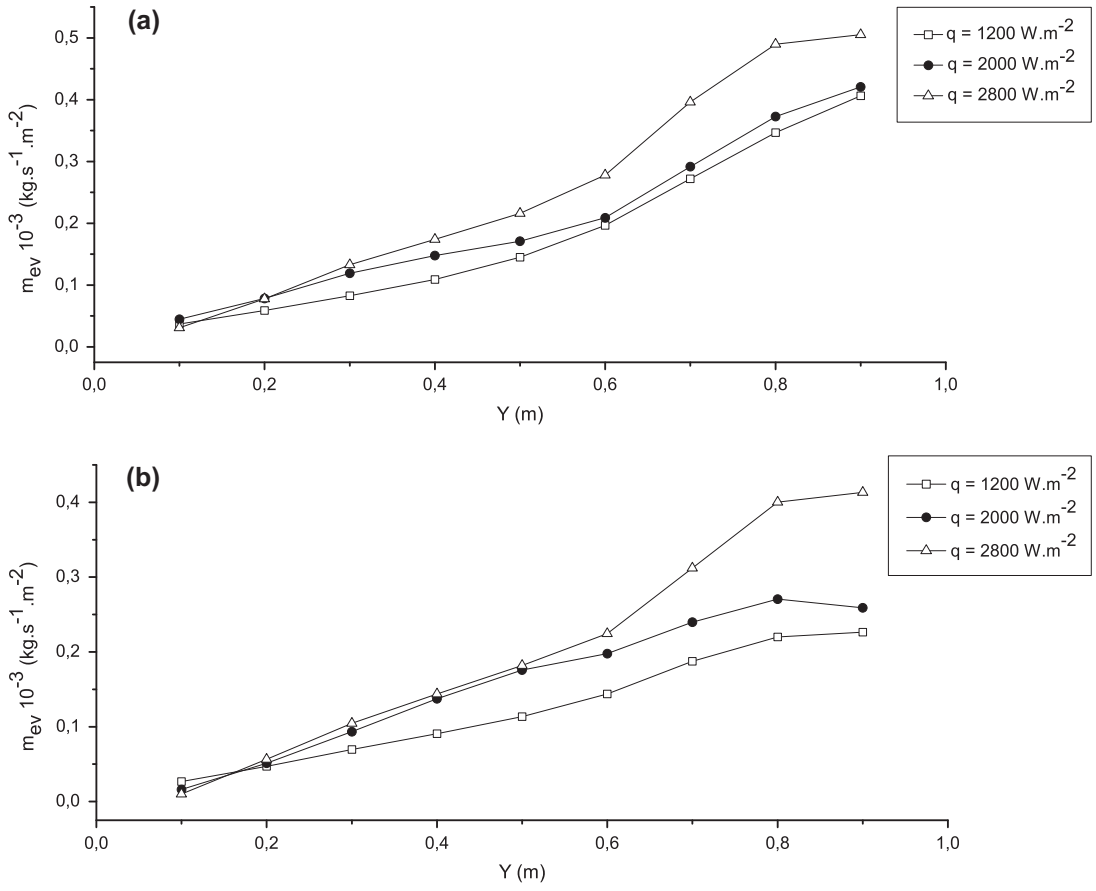

Fig. 11. Evolution of the local evaporated flow rate (a. $m_{in} = 2.77$ g m^{-2} s^{-1}) (b. $m_{in} = 4.44$ g m^{-2} s^{-1}).

DOI : 10.1016/j.enconman.2016.07.085

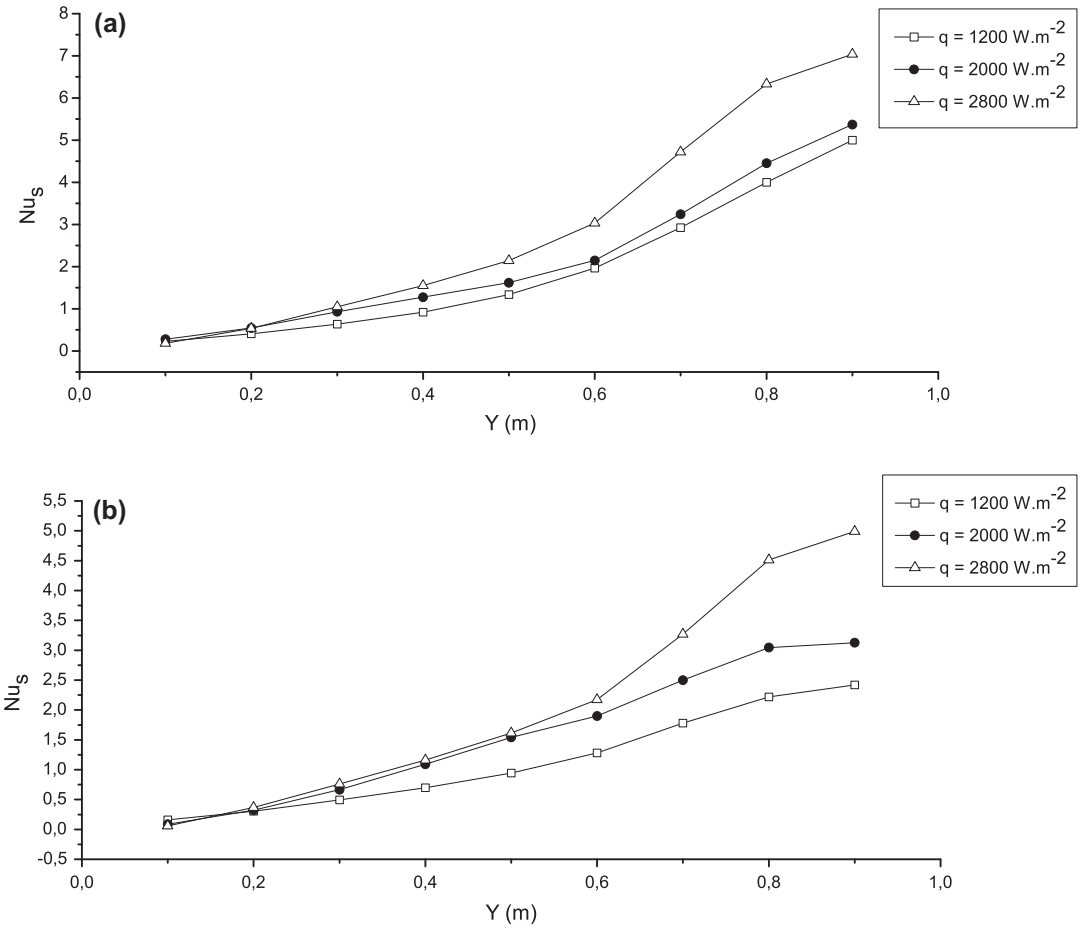

Fig. 12. Evolution of the local sensible Nusselt number (a. $m_{in} = 2.77$ g m^{-2} s^{-1}) (b. $m_{in} = 4.44$ g m^{-2} s^{-1}).

liquid inlet flow, decreases the evaporated flow rate. This effect is explained by the fact that the contact time between the film and the heated plate is shorter when the inlet flow is important. So we can conclude that to upgrade evaporation, the system must operate at low water inlet flow, which is consistent with the results of Cherif et al. [9] who realised an experimental study on the natural and forced convection evaporation of a thin liquid film that flows on the inner faces of the plates of a vertical channel.

We also note that the calculated values of the local evaporated flow rates are more important in the outlet of the channel, which respects the temperature profile and confirms the existence of both heating and evaporation zones. Indeed, the liquid is heated progressively without notable evaporation. Then, the temperature stabilizes and the evaporated flow rates become important.

In order to generalize our study, heat and mass transfer along the plate were described by dimensionless numbers. The transfer of heat exchanged at the interface between the film of water and air is the sum of the convective flux and latent flux [35]:

$$\phi_T = \phi_S + \phi_L \tag{5}$$

The local Nusselt number at the interface is defined as:

$$Nu = \frac{\phi_T}{\phi_{cd}} \tag{6}$$

May be consisted of two dimensionless numbers:

$$Nu = Nu_s + Nu_L \tag{7}$$

where Nu_s and Nu_L represent the sensible local Nusselt number and the latent local Nusselt number, describing respectively the sensible and latent transfer:

$$Nu_s = \frac{\phi_S L}{\lambda(T_p - T_{l_i n})} \tag{8}$$

$$Nu_L = \frac{\phi_L L}{\lambda(T_p - T_{l_i n})} \tag{9}$$

Fig. 12 represents the variation of the sensible local Nusselt number throughout the plate, for different heat flux and different liquid inlet flows. Same as the evaporated flow, we note that the sensible Nusselt number increases with the increase of the heat flow and the decrease of the liquid inlet flow. This result is in agreement with the work of Fahem et al. [10] who conducted a numerical analysis on the heat and mass transfer within a distillation cell.

We represent in Fig. 13 the variation of the latent local Nusselt number along the plate for different heat flux and different liquid inlet flows. We note that the latent Nusselt number increases with increasing the heat flow and decreasing the liquid inlet flow. We also note that the latent Nusselt number is more important than the sensible Nusselt number. The flow dissipated by evaporation is greater than that used by the film to increase its temperature.

We present in Fig. 14 the evolution of the average velocity of the humid air for different heat flows and for two liquid inlet flows. In fact, the acceleration of the humid air within the channel caused by the buoyancy forces leads to an upward flow of vapor in the channel: It is the chimney effect. Vapor escapes from the top and creates a decrease in pressure which produces an aspiration of fresh air from the bottom of the channel to inwards. Observing Fig. 12, we note that the velocity increases with increasing the heat flow and reducing the water feed rate. As we have already mentioned,

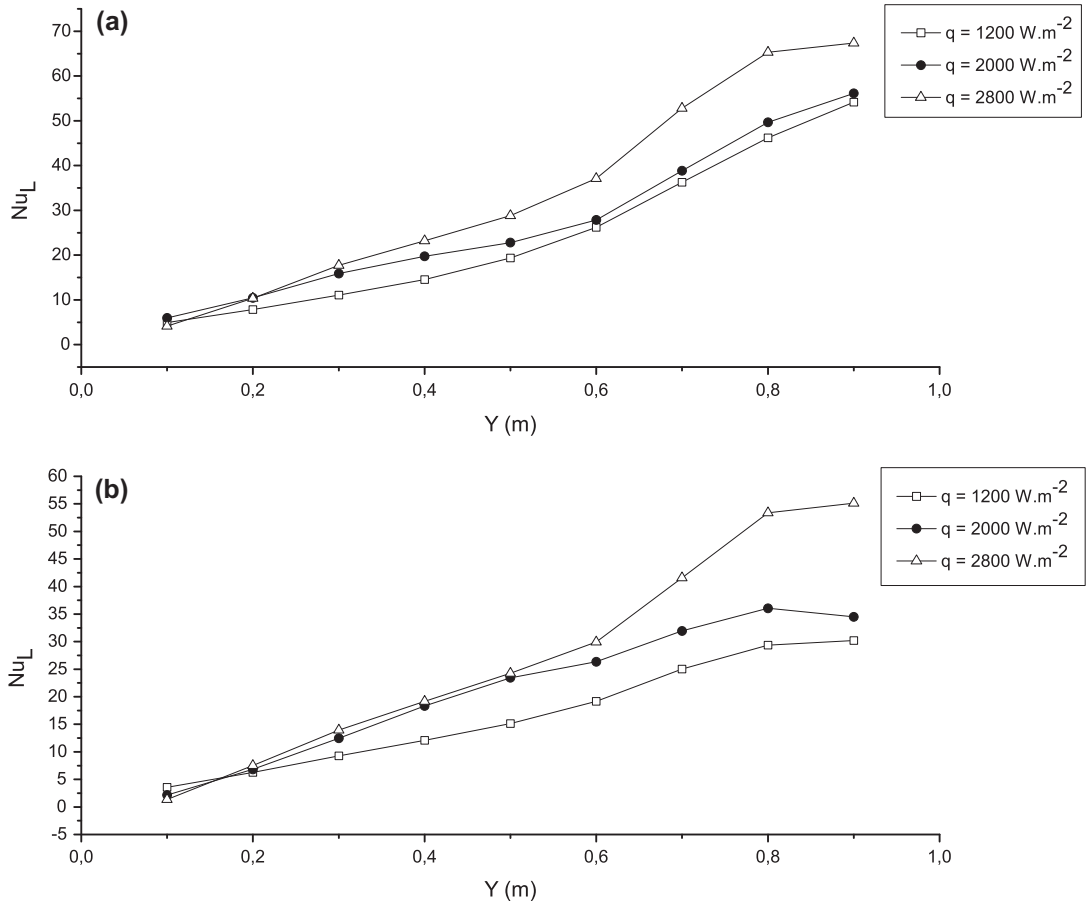

Fig. 13. Evolution of the local latent Nusselt number (a. $m_{in} = 2.77$ g m^{-2} s^{-1}) (b. $m_{in} = 4.44$ g m^{-2} s^{-1}).

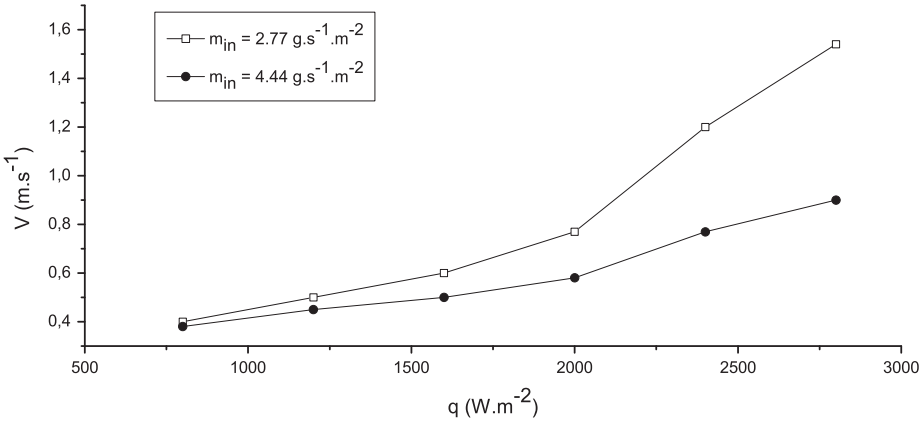

Fig. 14. Evolution of the average velocity of the humid air inside the channel.

the evaporated flow rate increases with increasing the heat flow and reducing the liquid inlet flow. The augmentation of the humidity in the channel explains the rise of the velocity as the water vapor is lighter than the dry air.

5. Conclusion

In this paper, we conducted an experimental study on the flow of a liquid film on one of the plates of a vertical channel. This plate was covered with a porous layer. With the realised experimental dispositif, we measured the temperature throughout the plate and the average evaporated flow rate. From these measurements, we solved the heat equation by inverse method which allowed us to determine the local variation of the evaporated flow rate, the latent Nusselt number and the sensible Nusselt number. The most significant conclusions are as follows:

1. The profile of the temperature is divided into two areas: the heating and the evaporation zones.
2. The use of the porous layer is more efficient in the case of a high heat flow.
3. To improve the evaporation, the system must operate at low water inlet flow.

DOI : 10.1016/j.enconman.2016.07.085

4. The latent Nusselt number is more important than the sensible one. The flow dissipated by evaporation is greater than the flow used by the film to increase its temperature.
5. The air velocity in the channel increases with increasing the evaporated flow rate.

References

[1] Cliche A, Lacroix M. Optimization of ice making in laminar falling films. Energy Convers Manage 2006;47:2260–70.
[2] Ronghui Q, Lina L, Yu H. Energy performance of solar-assisted liquid desiccant air-conditioning system for commercial building in main climate zones. Energy Convers Manage 2014;88:749–57.
[3] Buker MS, Mempouo B, Riffat SB. Experimental investigation of a building integrated photovoltaic/thermal roof collector combined with a liquid desiccant enhanced indirect evaporative cooling system. Energy Convers Manage 2015;101:239–54.
[4] Moshari S, Heidarinejad G, Fathipour A. Numerical investigation of wet-bulb effectiveness and water consumption in one-and two-stage indirect evaporative coolers. Energy Convers Manage 2016;108:309–21.
[5] Raimundo AM, Gaspar AR, Virgilio A, Divo MO, Quintela A. Wind tunnel measurements and numerical simulations of water evaporation in forced convection airflow. Int J Therm Sci 2014;86:28–40.
[6] Siow EC, Ormiston SJ, Soliman HM. Fully coupled solution of a two-phase model for laminar film condensation of vapor gas mixtures in horizontal channels. Int J Heat Mass Transf 2002;45:3689–702.
[7] Yuan ZX, Yan XT, Ma CF. A study of coupled convective heat and mass transfer from thin water film to moist air flow. Int Commun Heat Mass Transf 2004;31:291–301.
[8] Ben Jabrallah S, Belghith A, Corriou JP. Convective heat and mass transfer with evaporation of a falling film in a cavity. Int J Therm Sci 2005;45:16–28.
[9] Cherif AS, Ben Jabrallah S, Corriou JP, Belghith A. Intensification of the liquid film evaporation in a vertical channel. Desalination 2010;250:433–7.
[10] Fahem K, Ben Jabrallah S, Belghith A, Corriou JP. Numerical simulation of the behaviour of a distillation cell with influence of the characteristics of the heating wall. Desalination 2006;201:185–97.
[11] Debbissi C, Orfi J, Ben Nasrallah S. Evaporation of water by free or mixed convection into humid air and superheated steam. Int J Heat Mass Transf 2003;46:4703–15.
[12] Min J, Tang Y. Theoretical analysis of water film evaporation characteristics on an adiabatic solid wall. Refrigeration 2015;53:55–61.
[13] Souza TR, Salvagnini WM, Camacho JLP, Taqueda MES. Performance of a solar energy powered falling film evaporator with film promoter. Energy Convers Manage 2008;49:3550–9.
[14] Jang J, Yan W, Huang C. Mixed convection heat transfer enhancement through film evaporation in inclined square ducts. Int J Heat Mass Transf 2005;48:2117–25.
[15] Yan W. Effects of film evaporation on laminar mixed convection heat and mass transfer in a vertical channel. Int J Heat Mass Transf 1995;38:1261–9.
[16] Aybar HS. Evaporation model of an inclined solar water distillation system. Desalination 2006;190:63–70.
[17] Zeghmati B, Daguenet M. Study of transient laminar free convection over an inclined wet flat plate. Int J Heat Mass Transf 1991;34:899–909.
[18] Agunaoun A, Daif A. Evaporation en convection forcée d un film mince s écoulant en régime permanent, laminaire et sans onde, sur une surface plane inclinée. Int J Heat Mass Transf 1994;18:2947–56.
[19] Cherif AA, Daif A. Etude numérique du transfert de chaleur et de masse entre deux plaques planes verticales en presence d un film de liquide binaire ruisselant sur l une des plaques chauffée. Int J Heat Mass Transf 1999;42:2399–418.
[20] Debbissi Hfaiedh C, Nasr A, Ben Nasrallah S. Evaporation of a binary liquid film flowing down the wall of two vertical plates. Int J Therm Sci 2013;72:34–46.
[21] Cherif AS, Kassim MA, Benhamou B, Harmand S, Corriou JP, Ben Jabrallah S. Experimental and numerical study of mixed convection heat and mass transfer in a vertical channel with film evaporation. Int J Therm Sci 2011;50:942–53.
[22] Debbissi Hfaiedh C, Nasr A, Ben Nasrallah S. Numerical study of heat and mass transfer from an inclined flat plate with wet and dry zones. Int J Heat Mass Transf 1992;35:2277–87.
[23] Gonda A, Lancereau P, Bondelier P, Luo L, Fan Y, Benezech S. Water falling film evaporation on a corrugated plate. Int J Therm Sci 2014;81:29–37.
[24] Zheng GS, Worek WM. Method of heat and mass transfer enhancement in film evaporation. Int J Heat Mass Transf 1996;39:97–108.
[25] Leu J, Jang J, Chou Y. Heat and mass transfer for liquid film evaporation along a vertical plate covered with a thin porous layer. Int J Heat Mass Transf 2006;49:1937–45.
[26] Chou Y, Yang R. The evaporation of a saturated porous layer inside an inclined airflow channel. Int J Heat Mass Transf 2007;28:407–17.
[27] Barford NC. Experimental measurement: precision, error and truth. second ed. New York: John Wiley and Sons; 1990.
[28] Lachheb M, Karkri M, Albouchi F, Mzali F, Ben Nasrallah S. Thermophysical properties estimation of paraffin/graphite composite phase change material using an inverse method. Energy Convers Manage 2014;82:229–37.
[29] Chou Y, Yang R. Inverse problem of estimating transient heat transfer rate on external wall of forced convection pipe. Energy Convers Manage 2008;49:2117–23.
[30] Gogoi TK, Pandey M, Das R. Estimation of operating parameters of a reheat regenerative power cycle using simplex search and differential evolution based inverse methods. Energy Convers Manage 2015;91:204–18.
[31] Tikhonov AN, Arsenin VY. Solution of ill-posed problems. V.H. Winston and Sons; 1977.
[32] Hadamard J. Lectures on Cauchy's problem in linear partial differential equations. Yale University Press; 1923.
[33] Etemad GA. Free convection heat transfer from a rotating horizontal cylinder to ambient air with interferometer study of flow. Am Soc Mech Eng 1954;77:1283–9.
[34] Beck JV, Blackwell B, Haji-Sheikh A. Comparison of some inverse heat conduction methods using experimental data. Int J Heat Mass Transf 1996;39:3649–57.
[35] Fedorov AG, Viskanta R, Mohamad AA. Turbulent heat and mass transfer in an asymmetrically heated, vertical parallel-plate channel. Int J Heat Fluid Flow 1997;18:307–15.